

Gibbs Ensemble Monte Carlo for Reactive Force Fields to Determine the Vapor–Liquid Equilibrium of CO₂ and H₂O

Koen Heijmans, Ionut C. Tranca, David M. J. Smeulders, Thijs J. H. Vlucht, and Silvia V. Gaastra-Nedea*

Cite This: *J. Chem. Theory Comput.* 2021, 17, 322–329

Read Online

ACCESS |

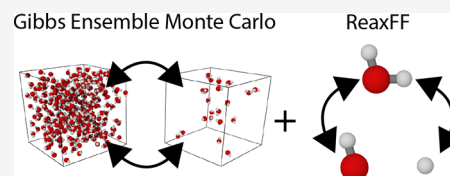
Metrics & More

Article Recommendations

Supporting Information

ABSTRACT: Absorption and reactive properties of fluids in porous media are key to the design and improvement of numerous energy related applications. Molecular simulations of these systems require accurate force fields that capture the involved chemical reactions and have the ability to describe the vapor–liquid equilibrium (VLE). Two new reactive force fields (ReaxFF) for CO₂ and H₂O are developed, which are capable of not only modeling bond breaking and formation in reactive environments but also predicting their VLEs at saturation conditions. These new force

fields include extra terms (ReaxFF-*lg*) to improve the long-range interactions between the molecules. For validation, we have developed a new Gibbs ensemble Monte Carlo (GEMC–ReaxFF) approach to predict the VLE. Computed VLE data show good agreement with National Institute of Standards and Technology reference data as well as existing nonreactive force fields. This validation proves the applicability of the GEMC–ReaxFF method to test new reactive force fields, and simultaneously it proves the applicability to extend newly developed ReaxFF force fields to other more complex reactive systems.



1. INTRODUCTION

In past decades, porous media such as metal–organic frameworks (MOFs), zeolitic imidazolate frameworks (ZIFs), and zeolites were intensively studied in combination with H₂O and CO₂.^{1–5} These studies have aimed to tackle challenges in many energy related applications such as water splitting,¹ sorption heat storage,⁶ CO₂ capture and sequestration,^{2,3,7} photoreduction,^{4,5} separation of natural gas mixtures,⁸ and syngas production.⁹ Within these fields, molecular simulations are frequently used to predict thermodynamic and kinetic properties.^{3,7,8,10–12} Molecular simulation is a useful tool for areas which are difficult or cumbersome to study using experimental approaches, and it simultaneously offers fundamental insights on the underlying physics of the simulated system on a micro/nanoscale.^{13–15}

The essential step for the successful use of molecular simulations is the development of a reliable force field, which is responsible for capturing relevant molecular interactions. Accurate force fields are required to reproduce the dynamic and static properties of a system. Furthermore, an important requirement for molecular studies of fluids in porous media is the correct description of the vapor–liquid equilibrium (VLE) by the force field.^{16,17} Numerous classical force fields have been developed, e.g., TIP4P/2005¹⁸ for H₂O and TraPPE¹⁹ for CO₂. By using such a force field, important properties such as the adsorption and diffusion of fluids in porous media^{11,12,20} and thermal behavior^{11,21} of materials can be predicted.

Classical force fields contain empirically based interatomic potentials to compute the energy between atoms based on their positions. The classical approximation is well-suited for noncovalent interactions between atoms, such as Coulombic, van der Waals, and angle-strain interactions. In practice, fitting the nonreactive classical force field parameters to the

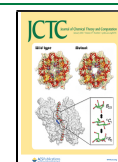
experimental VLE is often the first and most important step.^{16,17} It is important to note that chemical reactions often cannot be described with these classical force fields. This is a serious limitation, as many of the previously mentioned applications include at some point chemical reactions of H₂O and/or CO₂.

Simulations that take into account the electronic structures of atoms, such as density functional theory (DFT), can be used to describe chemical reactions. The downside of DFT approaches is the computational cost, and therefore these simulations are limited to small systems and short time scales.

Reactive force fields (ReaxFF), developed by van Duin et al.,^{22,23} aim to bridge the gap between DFT and classical force fields. The interatomic ReaxFF potentials are empirically based, like the classical force fields, thereby gaining computational advantages compared to DFT. Besides the conventional classical interaction potentials, connection-dependent/bond-order potentials²⁴ are included. The connection-dependent potentials allow ReaxFF to capture chemical reactions and open the way to model the dynamics of more complex multiphase processes,²⁴ without the need for expensive DFT calculations. Despite the importance of reactive force fields, to the best of our knowledge, there is no available ReaxFF force field which is able to accurately capture simultaneously the liquid, vapor, and

Received: August 24, 2020

Published: December 22, 2020



transition phases of H₂O and CO₂. In this work, we parametrized two new ReaxFF force fields, one for H₂O and one for CO₂, and used these to predict the VLEs of these specific systems.

For the parametrization of ReaxFF, most often DFT data is used as a reference. Both methods focus at first instance on short-range interactions in order to capture the (short-range) chemical reactions. This causes a less accurate description of the long-range interactions in the simulated system. It is well-known that long-range dispersion interactions are crucial for an accurate description of VLEs.¹⁵ In basic DFT, extra corrections are available, such as the DFT-D method of Grimme et al.²⁵ and the low-gradient (lg) method of Liu et al.,²⁶ to include these long-range dispersion interactions. The dispersion correction in DFT studies resulted in significantly improved descriptions of liquids at saturation conditions and predicted more accurate liquid properties.^{27,28} Similar to the lg method, Liu et al. developed an analogous extension for standard ReaxFF, named ReaxFF-lg.²⁹ This is a more sophisticated approach than basic ReaxFF due to the inclusion of the long-range London dispersion interactions, and it prevents modifications of the existing short-range (reactive) interactions. Here, we used this ReaxFF-lg methodology for the new force fields in order to correct for these long-range interactions. This enables the accurate reproduction of the phase diagrams for both H₂O and CO₂ and at the same time preserve the reactive properties.

The Gibbs ensemble Monte Carlo (GEMC) method is a comprehensive method to predict the VLE^{13–15} and has been used for many nonreactive systems.^{8,19,30,31} Accordingly, a new GEMC–ReaxFF method was developed to be used to study VLEs in combination with reactive systems. Our GEMC–ReaxFF approach allowed us to validate the new ReaxFF-lg H₂O and CO₂ force fields. The results were compared with experimental National Institute of Standards and Technology (NIST) reference data,^{32,33} confirming the ability of the GEMC–ReaxFF method to predict equilibria in reactive systems.

2. METHODOLOGY

Two new ReaxFF force fields were developed, for H₂O and CO₂, which allows the study of these fluids in reactive systems. To validate the new force fields, their VLEs were studied using a new method which was designed to combine the reactive force field molecular dynamics approach with Gibbs ensemble Monte Carlo^{13–15} (ReaxFF–GEMC). In the following sections, the ReaxFF, ReaxFF training, and GEMC methods are explained.

2.1. ReaxFF. The mathematical formulation that describes the forces between particles is called a force field. Force fields describe different kinds of interactions between atoms, which together add up to the potential energy of the system. When only classical forces are described, the force field is considered as a classical or nonreactive force field. Typically, the classical formulation of the van der Waals interactions is described by a Lennard-Jones potential, and an electrostatic force is described by Coulomb terms,^{18,19} which are respectively the first and second terms on the right-hand side of the following equation for the total interaction potential between atoms *i* and *j*:

$$U(r_{ij}) = 4\epsilon_{ij} \left[\left(\frac{\sigma_{ij}}{r_{ij}} \right)^{12} - \left(\frac{\sigma_{ij}}{r_{ij}} \right)^6 \right] + \frac{q_i q_j}{4\pi\epsilon r_{ij}} \quad (1)$$

where r_{ij} is the interatomic distance; ϵ_{ij} , σ_{ij} , q_i , and q_j are parametrized values of the Lennard-Jones energy parameter, Lennard-Jones size parameter, and partial charges for atoms *i* and *j*, respectively. ϵ is the electric constant. In classical force fields, bonds within molecules are typically considered as rigid^{18,19} or described with harmonic terms. This is a practical approach that simplifies the force field and speeds up simulations, and when applied to a nonreactive region it does not result in major accuracy losses. However, when one is interested in a region where chemical reactions can occur, these classical force fields fail because the intramolecular bonds cannot be broken. The reactive force field method (ReaxFF)^{22,23} aims to solve this problem by including bond breaking and formation terms. ReaxFF has proven its success for a wide range of reactive dynamics,²⁴ which were studied without requiring expensive DFT dynamics.

Similar to classical force fields, the ReaxFF potential is a summation of different energy terms:

$$E_{\text{system}} = E_{\text{vdW}} + E_{\text{Coul}} + E_{\text{bond}} + E_{\text{val}} + E_{\text{pen}} + E_{\text{under}} \\ + E_{\text{over}} + E_{\text{tors}} + E_{\text{conj}} + E_{\text{others}} \quad (2)$$

The nonbonded terms E_{vdW} and E_{Coul} are respectively the van der Waals and Coulomb contributions, which are considered between all atoms. The van der Waals interaction are described with a distance-corrected Morse potential, and the Coulomb interactions are described with a shielded Coulomb potential. The atomic charges are calculated with the electron equilibration method.^{34,35} The E_{bond} term accounts for the bond energy of the σ , π , and $\pi\pi$ bonds, and it is directly related to interatomic distances. When atoms are bonded, the intramolecular terms E_{under} , E_{over} , E_{val} , E_{tors} , E_{pen} , and E_{conj} can be used to correct for under- and overcoordination, valence and torsion angle terms, “penalty” energies, and conjugated systems, respectively. The E_{others} term can be added to include other interactions such as H-bonds. A more detailed explanation of these different terms can be found in the original paper of van Duin et al.²² It is important to note that the interatomic potentials are described in such a way that they are independent of the environment of the atom, which is required to allow chemical reactions (e.g., there is no difference between hydrogen atoms in H₂, H₂O, or a MgH₂ crystal).

To accurately capture the VLEs, long-range interactions play a key role.^{15,27,28} This is reflected in the practical assumption of using nonreactive classical force fields in most GEMC simulations. In the ReaxFF potential, long-range van der Waals interactions (E_{vdW}) are captured using a Morse potential, including a short-range repulsive part for the Pauli repulsion and a long-range attractive part for the van der Waals attractions. Historically, the main focus of ReaxFF is the short-range intramolecular dynamics; therefore, the Morse potential parameters are rather focused on these short-range interactions than on the long-range ones. Most training of ReaxFF is based on density functional theory (DFT), which suffers from similar phenomena. To adequately capture the long-range London dispersion interactions, standard DFT does not rely on first-principle methods, but uses empirical methods, such as the DFT-D method of Grimme et al.²⁵ and the low-gradient (lg) method of Liu et al.²⁶ To solve this issue for ReaxFF, an extended method (ReaxFF-lg) was developed by Liu et al.,²⁹ to improve the description of long-range interactions of ReaxFF. This method adds an extra term to the ReaxFF potential which is analogous to the low-gradient part for DFT. By adding this extra

term for the long-range interactions, an extensive refitting of the original vdW parameters in the Morse potential is avoided. Thereby, the original short-range reactive interactions remain intact, and a transferability similar to that for the original force field can be expected regarding chemical reactions. The additional lg term of the long-range interactions scales with $1/r_{ij}^6$:

$$E_{\text{lg}} = - \sum_{ij, i < j}^N \frac{C_{\text{lg},ij}}{r_{ij}^6 + dR_{e,ij}^6} \quad (3)$$

where $C_{\text{lg},ij}$ is the dispersion energy correction between atoms i and j . $R_{e,ij}$ is the equilibrium vdW radius between the atoms, and d is a scaling factor. The vdW radii are taken from previous a study²⁹ based on the universal force field (UFF).³⁶

2.1.1. ReaxFF Parametrization. To develop new reactive force fields for CO₂ and H₂O, two existing force fields were used as the starting point. The ReaxFF developed by Chenoweth et al.²³ for the simulation of hydrocarbon oxidation was chosen as the starting point for the new ReaxFF-lg for CO₂. The ReaxFF developed by Pathak et al.¹¹ for the simulation of salt hydrates was chosen as the starting point for the new H₂O ReaxFF-lg, which fundamentally showed an accurate description of water at different temperatures.³⁷ These original force fields have already proved their ability to correctly describe chemical reactions.^{11,23} However, as a consequence of their focus on hydrocarbon oxidation and chemical bonding in salt hydrates, these force fields lack the ability to accurately predict the VLE. An example of the different contributing long-range energies, for the different nonreactive and reactive force fields, will be shown and discussed in Figure 2 and Results.

To (re)parametrize some of the force field parameters, such as the newly added lg parameters, the Metropolis Monte Carlo (MMC) force field optimizer was used, which has proved itself for multiple force fields.^{11,38,39} The MMC optimizer, developed by Iype et al.,³⁹ is a high-dimensional and efficient training method, based on the simulated annealing Metropolis algorithm,^{40–43} and aimed to minimize the cumulative error between a data set and the predicted results by ReaxFF:

$$\text{Error}_{\text{new}} = \sum_{i=1}^n \left[\frac{X_{\text{ref},i} - X_{\text{ReaxFF},i}}{\sigma_i} \right] \quad (4)$$

with $X_{\text{ref},i}$ as the reference data (e.g., charges, energies, distances, heat of formation), $X_{\text{ReaxFF},i}$ as corresponding estimated values by ReaxFF, and a weighting factor σ_i for each data point i . The MMC optimizer searches the global minimum of the cumulative error, by modifying each iteration a random fraction of some selected parameters in a random direction. After each modification, $\text{Error}_{\text{new}}$ is calculated with the modified parameters, and the new force field is accepted according to

$$P = \min[1, \exp[-\beta(\text{Error}_{\text{new}} - \text{Error}_{\text{old}})]] \quad (5)$$

β is the reciprocal of the thermodynamic temperature $\beta = 1/(k_{\text{B}}T)$, k_{B} is the Boltzmann constant, and T is the artificial temperature. If the modifications are accepted, $\text{Error}_{\text{new}}$ becomes $\text{Error}_{\text{old}}$.

As training data sets, for both force fields, multiple reference configurations were used. For intramolecular interactions, the ADF software package⁴⁴ was used to generate reference data, and single gas molecules were fully relaxed to establish bond lengths, bond angles, and charges. The reference molecule for the prediction of charges was equilibrated at every iteration of

the MMC optimizer. To improve the long-range interactions, e.g., the newly added ReaxFF-lg parameters, reference configurations were generated by the TraPPE¹⁹ (CO₂) and TIP4P/2005¹⁸ (H₂O) classical force fields, due to their accurate description of VLEs.^{19,31} This set of reference configurations consisted of multiple sets of controlled trajectories of dimers, MD trajectories of near dimers, and MD trajectories at different densities spanning the entire saturation density. A representation of the training data set is given in the Supporting Information. The MMC optimizer ran multiple times, up to 20 000 iterations, with a slowly decreasing simulated annealing temperature, and including some final iterations to minimize the best generated set of parameters. The target acceptance rate was set to 10%, with a maximum acceptance rate of 70%.

2.2. Gibbs Ensemble Monte Carlo. The Gibbs ensemble Monte Carlo (GEMC) algorithm is a method for the direct simulation of gas–liquid phase coexistence, and was first introduced by Panagiotopoulos et al.^{13,14} GEMC simultaneously models the gas and liquid phases in two different simulation boxes, as shown in Figure 1. Both boxes start with

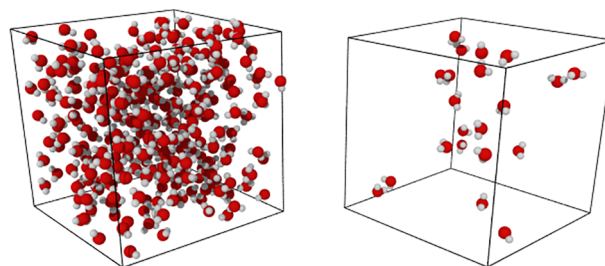


Figure 1. Examples of liquid and gas boxes in GEMC simulations. Besides thermalization, the two boxes can exchange molecules and volume.

a given number of molecules, a given volume, and thus a given density. During the simulation, molecules and volume are exchanged between the two boxes. One box will equilibrate to the gas phase and the other to the liquid phase. As a result, the phase coexistence of a fluid is modeled, at a given temperature and pressure, without an interfering interface between the phases. The Gibbs ensemble provides accurate coexistence densities for relatively small systems, provided that one is not too close to the critical point.¹⁵

The basic GEMC algorithm includes three types of trial moves, from which every cycle one will be randomly selected. The combination of these three trial moves allows the sampling of the entire phase space. Besides trial moves for thermalization, trial moves to exchange molecules and volume between the boxes are carried out. After each trial move the new energy of the total system is calculated, and on the basis of the acceptance rules (eqs 6 and 7) the trial move is accepted or rejected. The probability for accepting a molecule exchange (e.g., remove from box 1 and insert in box 2) is given by¹⁵

$$\text{acc}(o \rightarrow n) = \min \left[1, \frac{n_1(V - V_1)}{(N - n_1 + 1)V_1} \exp(-\beta[U_n - U_o]) \right] \quad (6)$$

where N , n_1 , V , and V_1 are the total number of molecules, number of molecules in box 1, total volume, and volume of box 1, respectively. U_n and U_o are the new and old potential energies of the simulation boxes. β is the reciprocal of the thermodynamic

temperature $\beta = 1/k_B T$, where k_B is the Boltzmann constant and T is the absolute temperature.

The probability for accepting volume exchange between the two boxes is given by¹⁵

$$\text{acc}(o \rightarrow n) = \min \left[1, \left(\frac{V_{n,1}}{V_{o,1}} \right)^{n_1+1} \left(\frac{V - V_{n,1}}{V - V_{o,1}} \right)^{N-n_1+1} \exp(-\beta[U_n - U_o]) \right] \quad (7)$$

During the GEMC simulation, the total number of molecules N and the total volume V remain constant.

For thermalization trial moves, one can perform Monte Carlo trial moves and translate/rotate each molecule separately. On the basis of the energy change ($U_n - U_o$), the thermalization is accepted or rejected. For convenience, we chose to perform a thermalization of all molecules in a single trial move by using a molecular dynamics (MD) algorithm. The MD is performed in the NVT ensemble with a Nosé–Hoover thermostat and a velocity Verlet integration scheme, using the SCM software package.⁴⁴ Each MD trajectory was performed for 625 fs, with a time step of 0.25 fs, which was sufficient to sample the system. The equilibrated NVT trajectory allowed us to accept every thermalization step and sample the entire phase space of the system.

The critical point of the VLE can be calculated using fitting with the law of rectilinear diameters:¹⁵

$$\frac{\rho_l + \rho_g}{2} = \rho_c + A \left(1 - \frac{T}{T_c} \right) \quad (8)$$

where ρ_l , ρ_g , and ρ_c are the liquid, gas, and critical density. T and T_c are the temperature and critical temperature. The density difference of the phases can be fitted to a scaling law:

$$\rho_l - \rho_g = B \left(1 - \frac{T}{T_c} \right)^\gamma \quad (9)$$

with γ as the critical exponent, which is $\gamma = 0.32$ for 3D systems. The parameters A and B are obtained from the fit.

3. RESULTS

3.1. ReaxFF-Ig_{CO₂} and ReaxFF-Ig_{H₂O} Validation. The MMC force field optimizer³⁹ was used to parametrize the new ReaxFF force fields. The scaling factor for the long-range interactions was set to $d = 1$, according to Liu et al.²⁹ Hence, regarding the long-range interactions, only the $C_{lg,ij}$ need to be fitted.

The resulting parameters are listed in Table 1, and full details on the new force fields are provided in the Supporting Information. Detailed results from the parametrizations, and comparisons between the different potentials, can also be found in the Supporting Information.

Table 1. ReaxFF-Ig Parameters of the New ReaxFF-Ig CO₂ and H₂O Force Fields

force field	atom	R_c (Å)	interaction	C_{lg} (kcal/mol·Å ⁶)
H ₂ O	O	1.75	O–O	142.9733
CO ₂	C	1.9255	C–C	249.5817
	O	1.75	O–O	14.9286
			O–C	127.1788

The resulting intramolecular geometric parameters and partial charges of the new ReaxFF-Ig are shown in Table 2, for CO₂ and

Table 2. Predicted ReaxFF Molecular Parameters for the Original and New Force Fields for CO₂ and H₂O

		CO ₂		
		orig ReaxFF ²³	ReaxFF-Ig _{CO₂}	TraPPE ¹⁹
bond distance (Å)	C–O	1.18	1.19	1.16
	O–C–O	180	180	180
charge (<i>e</i>)	C	+0.459	+0.693	+0.70
	O	−0.244	−0.346	−0.35
		H ₂ O		
		orig ReaxFF ¹¹	ReaxFF-Ig _{H₂O}	TIP4P/2005 ¹⁸
bond distance (Å)	O–H	0.948	0.974	0.9572
	H–O–H	102.4	102.6	104.5
charge (<i>e</i>)	O	−0.619	−0.648	–
	H	+0.310	+0.324	+0.5664
	M	–	–	−1.1328

H₂O. The bond distances and angles from ReaxFF-Ig follow from a geometry optimization and are compared with the descriptions from the classical force fields.^{18,19} For these classical force fields, the bond angles and distances are fixed. The negative charge of the TIP4P/2005 water molecule is located at the fourth interaction site, called “M”, which is coplanar to the O–H–O atoms, at a distance of 0.1546 Å from the oxygen atom. Within the ReaxFF format the atomic charges follow from the numerical charge calculations with the electron equilibration method.^{34,35} As shown in the Table 2, the bond lengths and bond angles are in close agreement with the reference values.

Different contributing intermolecular energies are shown in Figure 2 for the separation of two parallel CO₂ molecules. Figure 2 shows close agreement among the nonreactive TraPPE force

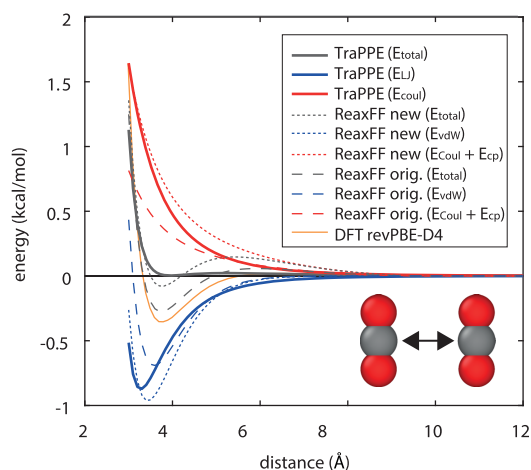


Figure 2. Comparison of different energy contributions regarding the dissociation of two parallel CO₂ molecules. The gray lines represent the total energy. The blue line represents the Lennard-Jones energy contribution for the TraPPE force field and the van der Waals energy for the ReaxFF force fields. The red line represents the Coulomb energy contribution for the TraPPE force field and the summation of the Coulomb and polarization energy in the ReaxFF force fields. The orange line represents the DFT-D reference.

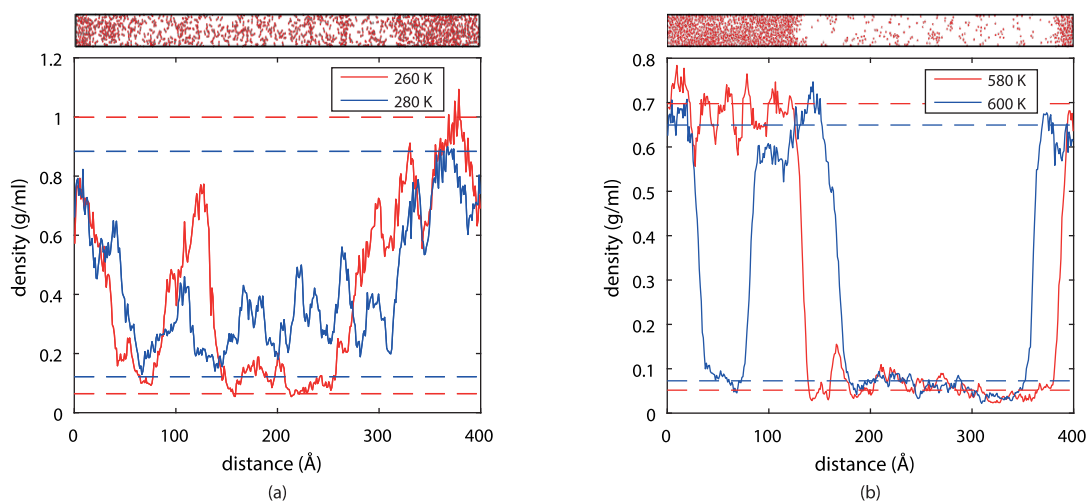


Figure 3. Average density distributions of the simulation boxes of (a) CO₂ and (b) H₂O after MD simulation. The red solid and dashed lines are the simulation results and the experimental coexistence densities^{32,33} for the lower temperatures, respectively. The blue solid and dashed lines are the simulation results and the experimental coexistence densities for the higher temperatures, respectively. The top boxes are representations of the final configurations at 280 and 580 K for CO₂ and H₂O, respectively.

field,¹⁹ competent in the prediction of the VLE, the original ReaxFF force field,²³ competent in the prediction of chemical reactions for hydrocarbon oxidation, and the new ReaxFF-Ig force field as a competent combination of the two. The differences between the red dashed lines are caused by the reparametrization of the ReaxFF parameters corresponding to the charge calculation. The differences between the blue dashed lines are caused by the added ReaxFF-Ig parameters. Both the van der Waals energy and Coulomb plus charge polarization energy increase in absolute value for the new ReaxFF-Ig force field compared to the original ReaxFF force field. It is clear that our new ReaxFF force field more closely matches the nonreactive TraPPE force field, compared to the original ReaxFF, especially at smaller distances. Furthermore, the summation of all the different contributing energies, represented by the gray lines, is more balanced around 0 and shows a less deep well for the new ReaxFF-Ig force field compared to the original. As a reference for the reactive component, the dimer interaction for two CO₂ molecules, obtained by DFT-D, is added. For this reference the revPBE⁴⁵ exchange–correlation function is used, which is an improved version of the PBE functional regarding molecules. For the dispersion interactions, Grimme’s latest dispersion correction D4⁴⁶ was used. The DFT-D dimer reference acknowledges the well depth for the ReaxFF force fields. Note that Figure 2 is a simplification of the system as only one of the infinite possibilities of CO₂ dimer interactions is considered. In the Supporting Information other dimer interactions, also used in the parametrization, can be found. Furthermore, for the DFT reference many different exchange–correlation functions and dispersion corrections can be used^{47,48} which could result in different curves.

The new ReaxFF-Ig CO₂ and H₂O force fields are tested, using MD, at coexistence conditions starting from a random initial configuration, and are equilibrated at temperatures just below their critical temperatures (at 260 and 280 K for CO₂ and at 580 and 600 K for H₂O). The resulting average density distributions (over 25 ps) are shown in Figure 3. From Figure 3, it is clear that the boxes equilibrate in partly liquid and partly gas phases. The overall plateaus of the density profiles (solid lines) are in the same range as experimental coexisting densities (dashed lines). The formation of the gas and liquid phases, separated by an

interface, is typically slow due to diffusion of the molecules. Eventually, the system will converge to a two-phase system.

3.2. GEMC–ReaxFF validation. To test the GEMC–ReaxFF approach, two simulations for H₂O were performed at 580 and 600 K with the new ReaxFF-Ig force field. The resulting densities of the simulation boxes are shown in Figure 4 and

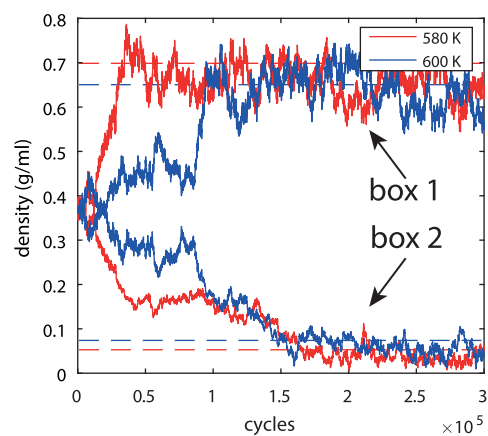


Figure 4. GEMC simulation of H₂O at 580 and 600 K. The solid lines represent the densities of the two boxes simulated by the GEMC–ReaxFF, with red at 580 K and blue at 600 K. The dashed lines represent experimental coexistence data.³³

compared with the experimental results.³³ It is clearly shown that, during the initialization of the system, one box equilibrates to liquid density and the other box equilibrates to gas density. Both densities are in good agreement with experimental values.³³

3.3. VLE with GEMC–ReaxFF. Because of moving droplets and interface effects, it is cumbersome to obtain accurate predictions of coexistence densities of the gas and liquid phases from Figure 3. With the use of a GEMC algorithm this is avoided, as each simulation box represents only liquid phase or only gas phase, and no interface is present between the phases. By use of the newly developed GEMC–ReaxFF method and force fields, we are able to determine the equilibrium phase diagram of H₂O and CO₂. After both the force fields and

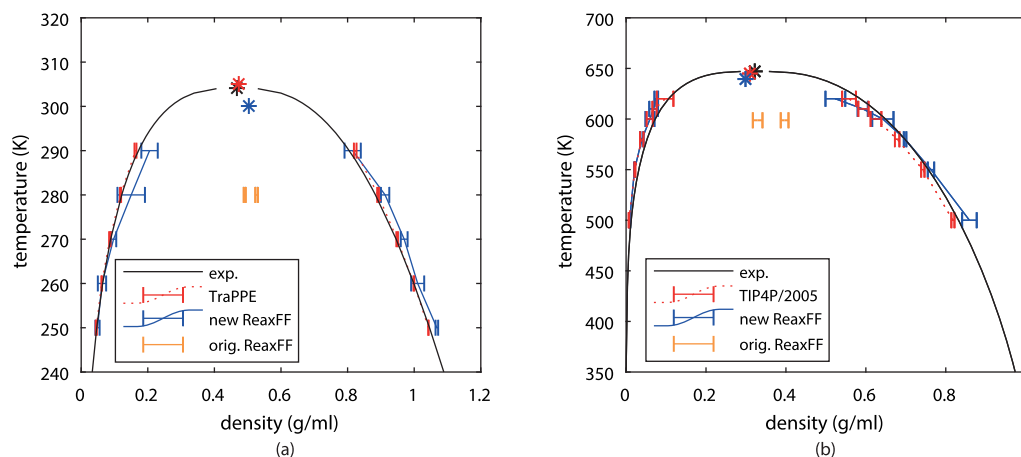


Figure 5. VLEs for (a) CO₂ and (b) H₂O. The black lines represent the NIST reference data. The red lines represent the (a) TraPPE force field and (b) TIP4P/2005 force field. The blue lines represent the predicted values by the new ReaxFF-*lg* force fields. The orange results represent the predicted by the original (a,¹¹ b²³) ReaxFF. The asterisks are the computed critical points using eqs 8 and 9

GEMC–ReaxFF code were validated (sections 3.1 and 3.2), their VLE was generated.

Each temperature was simulated with five different starting configurations. After equilibration, ensemble averages were taken for each simulation over 200 000 Monte Carlo cycles, resulting in a total of 1 000 000 cycles per temperature. All long-range interactions are computed with a taper function in combination with a 10 Å cutoff radius. For the CO₂ simulations, a total of 300 molecules were used; for the H₂O simulations, a total of 320 molecules were used.

The CO₂ results are compared with the TraPPE¹⁹ classical force fields. For these simulations the RASPA software package was used,^{49,50} with 1 000 000 cycles, 156 molecules, a cutoff distance of 10 Å including analytic tail corrections, and the Lorentz–Berthelot mixing rules. The H₂O results are compared with the TIP4P/2005¹⁸ classical force field, using 100 000 cycles, 360 molecules, and a cutoff distance of 12 Å including analytic tail corrections. The corresponding VLEs for the different force fields are shown in Figure 5.

As a reference, GEMC–ReaxFF calculations with the original ReaxFF force fields are included at a single temperature and a limited number of cycles. These results show the need for the (re)parametrization regarding the VLE. The original ReaxFF,²³ aimed at hydrocarbon oxidations, converges the two boxes to similar densities at 280 K. Thereby, it underestimates the critical point, where its prediction can be even lower than 280 K. The original H₂O ReaxFF¹¹ shows a similar behavior, underpredicts the critical temperature, and shows only a slight difference between the densities in the two simulation boxes at 600 K.

Except for the original ReaxFF force fields, the critical temperatures and densities for CO₂ and H₂O are computed using eqs 8 and 9 and are listed in Table 3. The critical temperatures of CO₂ are 300, 305, and 304 K for the new ReaxFF, the classical TraPPE force field,¹⁹ and experiments,³² respectively. The critical temperatures of H₂O are 639, 645, and 647 K for the new ReaxFF, the classical TIP4P/2005 force field,¹⁸ and experiments,³³ respectively. The critical densities of CO₂ are 0.50, 0.47, and 0.47 g/mL for the new ReaxFF, the classical TraPPE force field,¹⁹ and experiments,³² respectively. The critical densities of H₂O are 0.30, 0.31, and 0.32 g/mL for the new ReaxFF, the classical TIP4P/2005 force field,¹⁸ and experiments,³³ respectively. The ReaxFF force fields show excellent results, only with a few percentages deviation from the

Table 3. Critical Points of CO₂ and H₂O^a

	CO ₂		
	ReaxFF- <i>lg</i> _{CO₂}	TraPPE ¹⁹	expt ³²
<i>T_c</i> (K)	300	305	304
<i>ρ_c</i> (g/mL)	0.50	0.47	0.47
	H ₂ O		
	ReaxFF- <i>lg</i> _{H₂O}	TIP4P/2005 ¹⁸	expt ³³
<i>T_c</i> (K)	639	645	647
<i>ρ_c</i> (g/mL)	0.30	0.31	0.32

^aComputed by eqs 8 and 9.

experiments. Moreover, the possibility is offered to include reactions in molecular simulations.

4. CONCLUSIONS

Two new reactive force fields were developed to capture the vapor–liquid equilibria for CO₂ and H₂O. Long-range dispersion interactions are key to accurately capturing the VLE with ReaxFF force fields. Therefore, an extended version of ReaxFF methodology, namely ReaxFF-*lg*, was used for the newly developed force fields. The parameters were optimized by using accurate DFT and classical force field data and the MMC optimizer. MD simulations, at saturation conditions, showed the applicability of the newly developed force fields. Additionally, the new ReaxFF force fields were validated using the newly developed GEMC–ReaxFF method, and the VLEs for both liquids were computed. The GEMC–ReaxFF method shows an excellent agreement between the experimental and the new ReaxFF VLEs. It is shown that ReaxFF-*lg* is capable of capturing both gas and liquid phases. The classical force fields from the literature slightly outperform the reactive force fields, but these classical force fields lack the applicability of capturing bond breaking and bond formation compared to the new ReaxFF force fields. The newly developed reactive force fields allow future studies on the effects of long-range interactions and chemical reactive events on fluid properties such as diffusion, surface tension, and viscosity. Additionally, the successful combination of GEMC and ReaxFF force fields allows the study of more complex systems such as binary systems for separation processes or loading of porous media with grand canonical Monte Carlo simulations. These topics and

implementations are not straightforward^{17,51,52} and, thereby, are outside the scope of this work. We feel that these are promising future research directions.

■ ASSOCIATED CONTENT

SI Supporting Information

The Supporting Information is available free of charge at <https://pubs.acs.org/doi/10.1021/acs.jctc.0c00876>.

ReaxFF_CO2: developed reactive force field of CO₂ (PDF)

ReaxFF_H2O: developed force field of H₂O (PDF)

MMC parametrization: comparison results of ReaxFF parametrization (PDF)

■ AUTHOR INFORMATION

Corresponding Author

Silvia V. Gaastra-Nedea – Department of Mechanical Engineering, Eindhoven University of Technology, 5600MB Eindhoven, The Netherlands; Email: s.v.nedea@tue.nl

Authors

Koen Heijmans – Department of Mechanical Engineering, Eindhoven University of Technology, 5600MB Eindhoven, The Netherlands; orcid.org/0000-0002-8940-935X

Ionut C. Tranca – Department of Mechanical Engineering, Eindhoven University of Technology, 5600MB Eindhoven, The Netherlands

David M. J. Smeulders – Department of Mechanical Engineering, Eindhoven University of Technology, 5600MB Eindhoven, The Netherlands

Thijs J. H. Vlugt – Process & Energy Department, Delft University of Technology, 2628CB Delft, The Netherlands; orcid.org/0000-0003-3059-8712

Complete contact information is available at: <https://pubs.acs.org/doi/10.1021/acs.jctc.0c00876>

Notes

The authors declare no competing financial interest.

■ ACKNOWLEDGMENTS

The authors thank The Netherlands Organization for Scientific Research (NWO) for access to the National High Performance Computing facilities Cartesius. K.H., I.C.T., and S.V.G.-N. acknowledge COST Action 18234. T.J.H.V. acknowledges NWO-CW for a VICI grant.

■ REFERENCES

- (1) Zhang, M.; Dai, Q.; Zheng, H.; Chen, M.; Dai, L. Novel MOF-derived Co@N-C bifunctional catalysts for highly efficient Zn-air batteries and water splitting. *Adv. Mater.* **2018**, *30*, 1705431.
- (2) Flaig, R. W.; Osborn Popp, T. M.; Fracaroli, A. M.; Kapustin, E. A.; Kalmutzki, M. J.; Altamimi, R. M.; Fathieh, F.; Reimer, J. A.; Yaghi, O. M. The chemistry of CO₂ capture in an amine-functionalized metal-organic framework under dry and humid conditions. *J. Am. Chem. Soc.* **2017**, *139*, 12125–12128.
- (3) Lin, L.-C.; Berger, A. H.; Martin, R. L.; Kim, J.; Swisher, J. A.; Jariwala, K.; Rycroft, C. H.; Bhowan, A. S.; Deem, M. W.; Haranczyk, M.; Smit, B. In silico screening of carbon-capture materials. *Nat. Mater.* **2012**, *11*, 633–641.
- (4) Liu, Y.; Yang, Y.; Sun, Q.; Wang, Z.; Huang, B.; Dai, Y.; Qin, X.; Zhang, X. Chemical adsorption enhanced CO₂ capture and photo-reduction over a copper porphyrin based metal organic framework. *ACS Appl. Mater. Interfaces* **2013**, *5*, 7654–7658.

- (5) Xie, Y.; Fang, Z.; Li, L.; Yang, H.; Liu, T.-F. Creating Chemisorption Sites for Enhanced CO₂ Photoreduction Activity through Alkylamine Modification of MIL-101-Cr. *ACS Appl. Mater. Interfaces* **2019**, *11*, 27017–27023.

- (6) Scapino, L.; Zondag, H. A.; Van Bael, J.; Diriken, J.; Rindt, C. C. Sorption heat storage for long-term low-temperature applications: A review on the advancements at material and prototype scale. *Appl. Energy* **2017**, *190*, 920–948.

- (7) Ramdin, M.; Balaji, S. P.; Vicent-Luna, J. M.; Gutierrez-Sevillano, J. J.; Calero, S.; de Loos, T. W.; Vlugt, T. J. H. Solubility of the precombustion gases CO₂, CH₄, CO, H₂, N₂, and H₂S in the ionic liquid [bmim][Tf₂N] from Monte Carlo simulations. *J. Phys. Chem. C* **2014**, *118*, 23599–23604.

- (8) Ramdin, M.; Jamali, S.; Becker, T.; Vlugt, T. J. H. Gibbs ensemble Monte Carlo simulations of multicomponent natural gas mixtures. *Mol. Simul.* **2018**, *44*, 377–383.

- (9) Rostrup-Nielsen, J. R. Production of synthesis gas. *Catal. Today* **1993**, *18*, 305–324.

- (10) Pathak, A. D.; Nedea, S.; Zondag, H.; Rindt, C.; Smeulders, D. Diffusive transport of water in magnesium chloride dihydrate under various external conditions for long term heat storage: A ReaxFF-MD study. *European Journal of Mechanics-B/Fluids* **2017**, *64*, 93–101.

- (11) Pathak, A. D.; Heijmans, K.; Nedea, S.; van Duin, A. C.; Zondag, H.; Rindt, C.; Smeulders, D. Mass diffusivity and thermal conductivity estimation of chloride-based salt hydrates for thermo-chemical heat storage: A molecular dynamics study using the reactive force field. *Int. J. Heat Mass Transfer* **2020**, *149*, 119090.

- (12) Poursaeidesfahani, A.; de Lange, M. F.; Khodadadian, F.; Dubbeldam, D.; Rigutto, M.; Nair, N.; Vlugt, T. J. H. Product shape selectivity of MFI-type, MEL-type, and BEA-type zeolites in the catalytic hydroconversion of heptane. *J. Catal.* **2017**, *353*, 54–62.

- (13) Panagiotopoulos, A. Z. Direct determination of phase coexistence properties of fluids by Monte Carlo simulation in a new ensemble. *Mol. Phys.* **1987**, *61*, 813–826.

- (14) Panagiotopoulos, A. Z.; Quirke, N.; Stapleton, M.; Tildesley, D. Phase equilibria by simulation in the Gibbs ensemble: alternative derivation, generalization and application to mixture and membrane equilibria. *Mol. Phys.* **1988**, *63*, 527–545.

- (15) Frenkel, D.; Smit, B. *Understanding Molecular Simulation*, 2nd ed.; Academic Press: London, U.K., 2002.

- (16) Matito-Martos, I.; Álvarez-Ossorio, J.; Gutiérrez-Sevillano, J.; Doblaré, M.; Martín-Calvo, A.; Calero, S. Zeolites for the selective adsorption of sulfur hexafluoride. *Phys. Chem. Chem. Phys.* **2015**, *17*, 18121–18130.

- (17) Garcia-Sanchez, A.; Ania, C. O.; Parra, J. B.; Dubbeldam, D.; Vlugt, T. J. H.; Krishna, R.; Calero, S. Transferable force field for carbon dioxide adsorption in zeolites. *J. Phys. Chem. C* **2009**, *113*, 8814–8820.

- (18) Abascal, J. L.; Vega, C. A general purpose model for the condensed phases of water: TIP4P/2005. *J. Chem. Phys.* **2005**, *123*, 234505.

- (19) Potoff, J. J.; Siepmann, J. I. Vapor-liquid equilibria of mixtures containing alkanes, carbon dioxide, and nitrogen. *AIChE J.* **2001**, *47*, 1676–1682.

- (20) Dubbeldam, D.; Calero, S.; Vlugt, T. J. H.; Krishna, R.; Maesen, T. L.; Smit, B. United atom force field for alkanes in nanoporous materials. *J. Phys. Chem. B* **2004**, *108*, 12301–12313.

- (21) Heijmans, K.; Pathak, A. D.; Solano-López, P.; Giordano, D.; Nedea, S.; Smeulders, D. Thermal boundary characteristics of homo-/heterogeneous interfaces. *Nanomaterials* **2019**, *9*, 663.

- (22) Van Duin, A. C.; Dasgupta, S.; Lorient, F.; Goddard, W. A. ReaxFF: a reactive force field for hydrocarbons. *J. Phys. Chem. A* **2001**, *105*, 9396–9409.

- (23) Chenoweth, K.; Van Duin, A. C.; Goddard, W. A. ReaxFF reactive force field for molecular dynamics simulations of hydrocarbon oxidation. *J. Phys. Chem. A* **2008**, *112*, 1040–1053.

- (24) Senftle, T. P.; Hong, S.; Islam, M. M.; Kylasa, S. B.; Zheng, Y.; Shin, Y. K.; Junkermeier, C.; Engel-Herbert, R.; Janik, M. J.; Aktulga, H. M.; Verstraelen, T.; Grama, A.; van Duin, A. C. T. The ReaxFF reactive

force-field: development, applications and future directions. *npj Comput. Mater.* **2016**, *2*, 15011.

(25) Grimme, S.; Antony, J.; Ehrlich, S.; Krieg, H. A consistent and accurate ab initio parametrization of density functional dispersion correction (DFT-D) for the 94 elements H-Pu. *J. Chem. Phys.* **2010**, *132*, 154104.

(26) Liu, Y.; Goddard, W. A., III First-principles-based dispersion augmented density functional theory: From molecules to crystals. *J. Phys. Chem. Lett.* **2010**, *1*, 2550–2555.

(27) McGrath, M. J.; Kuo, I.-F. W.; Ghogomu, J. N.; Mundy, C. J.; Siepmann, J. I. Vapor–liquid coexistence curves for methanol and methane using dispersion-corrected density functional theory. *J. Phys. Chem. B* **2011**, *115*, 11688–11692.

(28) Baer, M. D.; Mundy, C. J.; McGrath, M. J.; Kuo, I.-F. W.; Siepmann, J. I.; Tobias, D. J. Re-examining the properties of the aqueous vapor–liquid interface using dispersion corrected density functional theory. *J. Chem. Phys.* **2011**, *135*, 124712.

(29) Liu, L.; Liu, Y.; Zybun, S. V.; Sun, H.; Goddard, W. A., III ReaxFF-lg: Correction of the ReaxFF reactive force field for London dispersion, with applications to the equations of state for energetic materials. *J. Phys. Chem. A* **2011**, *115*, 11016–11022.

(30) Ramdin, M.; Becker, T. M.; Jamali, S. H.; Wang, M.; Vlugt, T. J. H. Computing equation of state parameters of gases from Monte Carlo simulations. *Fluid Phase Equilib.* **2016**, *428*, 174–181.

(31) Vega, C.; Abascal, J.; Nezbeda, I. Vapor-liquid equilibria from the triple point up to the critical point for the new generation of TIP4P-like models: TIP4P/Ew, TIP4P/2005, and TIP4P/ice. *J. Chem. Phys.* **2006**, *125*, 034503.

(32) Span, R.; Wagner, W. A new equation of state for carbon dioxide covering the fluid region from the triple-point temperature to 1100 K at pressures up to 800 MPa. *J. Phys. Chem. Ref. Data* **1996**, *25*, 1509–1596.

(33) Wagner, W.; Prueß, A. The IAPWS formulation 1995 for the thermodynamic properties of ordinary water substance for general and scientific use. *J. Phys. Chem. Ref. Data* **2002**, *31*, 387–535.

(34) Mortier, W. J.; Ghosh, S. K.; Shankar, S. Electronegativity-equalization method for the calculation of atomic charges in molecules. *J. Am. Chem. Soc.* **1986**, *108*, 4315–4320.

(35) Janssens, G. O.; Baekelandt, B. G.; Toufar, H.; Mortier, W. J.; Schoonheydt, R. A. Comparison of cluster and infinite crystal calculations on zeolites with the electronegativity equalization method (EEM). *J. Phys. Chem.* **1995**, *99*, 3251–3258.

(36) Rappé, A. K.; Casewit, C. J.; Colwell, K.; Goddard, W. A., III; Skiff, W. M. UFF, a full periodic table force field for molecular mechanics and molecular dynamics simulations. *J. Am. Chem. Soc.* **1992**, *114*, 10024–10035.

(37) Iype, E. In *Silico Characterisation of Magnesium Salt Hydrates as Energy Storage Materials*. Ph.D. Thesis, Eindhoven University of Technology, 2014. DOI: 10.6100/IR770079.

(38) Pathak, A. D.; Nedeá, S.; Van Duin, A. C.; Zondag, H.; Rindt, C.; Smeulders, D. Reactive force field development for magnesium chloride hydrates and its application for seasonal heat storage. *Phys. Chem. Chem. Phys.* **2016**, *18*, 15838–15847.

(39) Iype, E.; Hütter, M.; Jansen, A.; Nedeá, S. V.; Rindt, C. Parameterization of a reactive force field using a Monte Carlo algorithm. *J. Comput. Chem.* **2013**, *34*, 1143–1154.

(40) Metropolis, N.; Rosenbluth, A. W.; Rosenbluth, M. N.; Teller, A. H.; Teller, E. Equation of state calculations by fast computing machines. *J. Chem. Phys.* **1953**, *21*, 1087–1092.

(41) Kirkpatrick, S.; Gelatt, C. D.; Vecchi, M. P. Optimization by simulated annealing. *Science* **1983**, *220*, 671–680.

(42) Pongsai, S. Combination of the Metropolis Monte Carlo and Lattice Statics method for geometry optimization of H-(Al)-ZSM-5. *J. Comput. Chem.* **2010**, *31*, 1979–1985.

(43) Caflisch, A.; Niederer, P.; Anliker, M. Monte Carlo minimization with thermalization for global optimization of polypeptide conformations in Cartesian coordinate space. *Proteins: Struct., Funct., Genet.* **1992**, *14*, 102–109.

(44) te Velde, G.; Bickelhaupt, F. M.; Baerends, E. J.; Fonseca Guerra, C.; van Gisbergen, S. J. A.; Snijders, J. G.; Ziegler, T. Chemistry with ADF. *J. Comput. Chem.* **2001**, *22*, 931–967.

(45) Zhang, Y.; Yang, W. Comment on "Generalized gradient approximation made simple. *Phys. Rev. Lett.* **1998**, *80*, 890.

(46) Caldeweyher, E.; Ehlert, S.; Hansen, A.; Neugebauer, H.; Spicher, S.; Bannwarth, C.; Grimme, S. A generally applicable atomic-charge dependent London dispersion correction. *J. Chem. Phys.* **2019**, *150*, 154122.

(47) Grimme, S. Density functional theory with London dispersion corrections. *Wiley Interdiscip. Rev.: Comput. Mol. Sci.* **2011**, *1*, 211–228.

(48) Rana, M. K.; Koh, H. S.; Hwang, J.; Siegel, D. J. Comparing van der Waals density functionals for CO₂ adsorption in metal organic frameworks. *J. Phys. Chem. C* **2012**, *116*, 16957–16968.

(49) Dubbeldam, D.; Calero, S.; Ellis, D. E.; Snurr, R. Q. RASPA: molecular simulation software for adsorption and diffusion in flexible nanoporous materials. *Mol. Simul.* **2016**, *42*, 81–101.

(50) Dubbeldam, D.; Torres-Knoop, A.; Walton, K. S. On the inner workings of Monte Carlo codes. *Mol. Simul.* **2013**, *39*, 1253–1292.

(51) Vlugt, T.; Martin, M.; Smit, B.; Siepmann, J.; Krishna, R. Improving the efficiency of the configurational-bias Monte Carlo algorithm. *Mol. Phys.* **1998**, *94*, 727–733.

(52) Orozco, G. A.; Economou, I. G.; Panagiotopoulos, A. Z. Optimization of intermolecular potential parameters for the CO₂/H₂O mixture. *J. Phys. Chem. B* **2014**, *118*, 11504–11511.